IDENTIFICATION OF POLYMERS IN WASTE TYRE REINFORCING FIBRE BY THERMAL ANALYSIS AND PYROLYSIS

B.Acevedo, A.M. Fernández, C. Barriocanal*
Instituto Nacional del Carbón, INCAR-CSIC, Apartado 73, 33080 Oviedo. Spain
*Corresponding author. Tel: +34 985 11 90 90; Fax:+34 985 29 76 62; e.mail address: carmenbr@incar.csic.es

ABSTRACT

The composition of the reinforcing fibre obtained from the recycling of scrap tyres was analyzed with a view to finding the most suitable applications for it. The material (RF) was separated into two different parts i.e. fibre (F) and microfibre (MF) to ensure the maximum homogeneity of the material under study. Thermogravimetric analysis (TG) together with differential scanning calorimetry (DSC) and infrared spectroscopy (FTIR) were used to identify the polymers present in the waste and to determine in what proportions they were present. Determination of the temperatures of maximum volatile matter evolution (Tmax), the yield at the end of the pyrolysis and the melting temperatures yielded very useful results for the identification of the polymers. In order to confirm the results obtained, pyrolysis of the pure polymers was carried out and the decomposition products were analysed. The results were then compared with the oil composition data derived from the pyrolysis of the waste fibres. Our results showed the presence of two polyamides, rayon, polyester and aramid.

Keywords: recycling, tyre reinforcing fibre, TG/DTG, DSC, GC-MS, polymer blends.

1. Introduction

Every year 1.2 billion scrap tyres are generated worldwide [1]. European legislation has established the following preferential order of environmental friendly management with respect to waste material: reduction, reuse, recycling and energy production. Waste reduction (or prevention) is the preferred approach to waste management because waste that is not created forestalls waste management costs. Moreover waste reduction also helps conserve resources for future generations and contributes to a cleaner environment. The percentage of tyres going to landfill has decreased in Europe drastically in recent years with a corresponding increase in the recovery of the materials as an alternative route for scrap tyre treatment [2]. The shredding of tyres is the normal mode of material recycling. In the process of size reduction, various fractions of rubber of different sizes are produced, together with steel and a product which is a fluff-like waste that is normally taken to landfill. This waste product is formed by textile fibres that are normally included in tyres as reinforcement. However, the main product of tyre recycling installations is rubber crumbs that are used in sports surfaces, as drainage material in roads or as an additive for asphalt. Apart from textile fibres, the fluff contains a certain amount of rubber that is difficult to separate. It has been reported [3] that tyre recycling plants produce, about 65%, 20% and 15% of crumb rubber, steel and waste fluff, respectively.

Three basic components are obtained from scrap tyres: rubber materials, steel and fibre. While there is a market for the rubber portions of the waste tyre, the steel and especially the fibre is more difficult to sell. Depending on the type of mechanical processing employed, steel is contaminated to varying degrees with rubber, making it more difficult to recycle. Compacted steel has a high value for the scrap steel processor. In the case of fibre, the problem is its great heterogeneity as it contains more than one type of textile. The presence of rubber and steel also make it extremely difficult to recycle.

Tyres are made of styrene-butadiene copolymer (SBR), natural rubber and poly-butadiene together with reinforcing materials (steel and polymeric fibres). All the materials

used are 100% recyclable. Moreover, their chemical and physical properties make them a highly valuable resource [4-6].

The pyrolysis of tyre rubber has been the subject of investigation for many years [5-10], in an attempt to find a use for its three main products (i.e. char, gas and oil). In addition the thermal decomposition of elastomers that are also present in tyre rubber has been studied in depth [11-14]. Yet so far the reinforcing fibre that is recovered as a waste in tyre shredding factories has received little attention [15-18]. The aim of the present work is to identify the fibres that are present in the waste recovered from tyre grinding factories to help in finding a use for this waste.

2. Materials and methods

2.1. Materials

The reinforcing fibre (RF) recovered from tyre recycling as a waste is a very heterogeneous product. It was therefore separated into two parts by sieving in order to improve the reproducibility of the results. One type of fibre made up of cords impregnated with rubber has been labelled simply fibre (F) with a size of approximately 18 mm x 10 mm x 4 mm, while the other type has been labelled microfibre, (MF), due to its appearance as a fluff and the presence of fine rubber crumbs stuck to it. Figure 1 shows an image of the two different components of the RF (i.e. F and MF), whose composition is thought to be different in view of their different mechanical behaviours in the process of scrap tyre size reduction. After the separation process RF was found to be composed of 54 wt.% of F and 46 wt.% of MF. Tyre rubber in the form of crumbs (TC) was also included in the study due to its presence in the composition of RF. The pure polymers used in this study were commercial grade polyester Dacron ® (Da), the polyamides Nylon 6 (Ny6) and Nylon 6,6 (Ny6,6), Rayon® (Ra) and aramid provided by Intexter (Spain). Proximate analyses were performed following the ISO562 and ISO1171 standard procedures for volatile matter and ash content, respectively. The elemental analysis was determined by means of a LECO CHN-2000 for C, H and N, a LECO S-144 DR for sulphur and a LECO VTF-900 for direct oxygen determination.

To be able to identify the polymers present in the reinforcing fibre, the analysis of F and MF was carried out using samples where the rubber had been eliminated by means of a sieve shaker machine that removes fine rubber particles. The elemental analysis of the cleaned F and MF has been included in Table S1.

2.2. Infrared spectroscopy

Fourier transform infrared spectroscopy (FTIR) spectra were recorded on a Nicolet Magna-IR560 spectrometer, an attenuated total reflectance (ATR) accessory being used to obtain the spectra of the fibre (F), the microfibre (MF) and the pure polymers. Data were collected in the range of 400 cm^{-1} to 4000 cm^{-1} with 32 scans for each sample. The resolution was 4 cm^{-1}.

2.3. Thermal analysis (TG/DTG/DSC)

The TG/DTG analysis of the fibre, microfibre, reinforcing fibre and pure polymers was carried out using a TA Instruments SDT Q600 thermoanalyser which allows the simultaneous detection of mass changes and heat effects during the decomposition of the samples. Samples of 10 mg were heated to 950 ℃ at a rate of 10 ℃/min under a nitrogen flow of 100 ml/min. From the data obtained by thermogravimetric analysis the volatile matter evolved up to a specific temperature (VMT) and the derivative of the weight loss curve (DTG curve) were calculated. In addition, Tmax, the temperature of maximum volatile matter evolution was derived from the TG/DTG curves. Differential scanning calorimetry (DSC) was carried out using the same equipment as that used for thermogravimetric analysis. Samples of 10 mg were heated up to 400 ℃ at 10 ℃/min. The tests were performed under a nitrogen flow of 100 ml/min. α-Alumina was the reference material used for the DSC measurements. Pt:Rh thermocouples placed at the bottom of the crucibles were used to measure the temperature which was calibrated with the melting peaks of high purity zinc, aluminium and silver. To calibrate the heat flow, sapphire was used. The melting point (T_m) was taken as the maximum of the endothermic peak.

2.3. Pyrolysis in a fixed bed horizontal oven (FB)

For each pyrolysis experiment a sample of 3-4 g of the reinforcing fibre (RF), the microfibre (MF), polyester Dacron ® (Da), the polyamides Nylon 6 (Ny6) and Nylon 6,6 (Ny6,6), Rayon® (Ra) was introduced into a cylindrical quartz reactor (32 cm long x 2.2 cm diameter) that was heated in a horizontal electrically-heated oven at 5 ℃/min to a final temperature of 850 ℃. During pyrolysis, the liquid products were collected using an ice-cooled trap. The char and liquid product yields were calculated relative to the starting material, while the gas yield was calculated by difference. The data reported is the average of at least two pyrolysis experiments.

2.4. Gas chromatographic analysis

Gas chromatographic analyses of tars were carried out on an Agilent Model 6890 Series II gas chromatograph equipped with flame ionization and mass spectrometry detection (GC-FID-MS). The separations were carried out using a fused-silica capillary column (HP-5MS) of length 30 m and I.D. 0.25 mm. The temperature was programmed from 50 to 295 ℃ at a rate of 4 ℃/min, the final tempe rature being held for 10 minutes. Helium was used as the carrier gas and split ratios of 1:200 and 1:50 were employed in the front (MS) and back (FID) injectors respectively. The detector and injector temperatures were 300 ℃ and the volume of sample injected was 1 µl.

3. Results and discussion

3.1. Main characteristics of the materials used

The proximate and elemental analysis results of the two main components (MF and F) separated from the as received reinforcing fibre are presented in Table 1 together with those of the reinforcing fibre (RF). Since the reinforcing fibre contains rubber, the main characteristics of the rubber (obtained at the same time from the same factory) have also been included in Table 1. From the proximate analysis it can be seen that MF presents the highest volatile matter content and lowest ash content. F presents values that are very similar to TC which would appear to indicate that the weight percentage of rubber present in F is higher than that of MF. Again, F shows an elemental composition that is similar to TC,

both of them exhibiting a high carbon content of around 78 wt.%db. In contrast MF has lower carbon content (57 wt.%db) but a higher oxygen content than F (31.2 vs. 7.8 wt.%). Because F has a higher carbon content, the C/H atomic ratio is higher for F than in the case of MF.

3.2. Infrared spectroscopy of fibres

Infrared spectroscopy is a very useful technique for identifying the type of bonds inside a molecule. For this reason it is commonly used to identify the functional groups present in polymers [19-25]. The pure polymers together with MF and F were studied by means of FTIR to see if the bands characteristic of pure polymers are present in MF and F. Table S2 displays the band assignment used to identify the characteristic bands. Figure 2.a shows the spectra corresponding to Da, Ra, polyamide and the MF. Various vertical lines have been drawn in the Figure to make it easier to identify the common bands. Da is an aromatic ester and so it presents three intense characteristic bands near 1720, 1245 and 1100 cm^{-1} which are due to C=O, C-C-O, O-C-C stretching respectively [19] and correspond to bands F, J and K in Figure 2.a. These characteristic bands are clearly observed in the spectrum of the microfibre. The spectrum of Ny6,6 and Ny6 present the same bands. Therefore only one has been included as an illustration. Ny6 is a secondary amide and this type of compound shows only one N-H stretching band in its infrared spectra, in this case at 3301 cm^{-1} (Band B in Figure 2.a). The bands at 2922 and 2855 cm^{-1} correspond to asymmetric and symmetric CH_2 stretching respectively (bands C and E in Figure 2.a). The C=O bond in the amides gives rise to strong C=O stretching bands. The conjugation between the carbonyl group and the amide nitrogen, causes the C=O stretching band to appear at a lower wavenumber than in ketones and esters [22]. In the present case a strong band appears at 1640 cm^{-1} (band G in Figure 2.a). The in-plane bending vibration of N-H in Ny6 appears at 1544 cm^{-1} (band H in Figure 2.a). Ra owes its presence to that of band K that is characteristic of the pure polymer. Figure 2.b shows the FTIR spectra of F together with the spectra corresponding to aramid, Da and Rayon. The bands characteristic of Da appear at 1720 cm^{-1}, 1245 cm^{-1} and 1100 cm^{-1} (bands F, J and K in Figure 2.b respectively), all of which appear in F. The most characteristic bands associated with aramide appear at 3301

cm^{-1} attributed to N-H stretching (band B in Figure 2.b), while another appears at 1640 cm-1 (band G in Figure 2.b) related to the stretching of the C=O bond and a third at 1544 (band H in Figure 2.b) due to the bending vibration of the N-H bond. In the spectrum of F the bands corresponding to Da and aramid are apparent. Ra is a derivative of cellulose and in the spectrum a broad band due to hydrogen-bonded OH stretching at ca. 3500-3200 cm^{-1} is observed together with C-H stretching at 2900 cm^{-1}, the C-H deformation vibration at 1375 cm^{-1} and the C-OC, C-C-O and C-C-H deformation modes and stretching vibrations in where the motions of the C-5 and C-6 atoms are at 900 cm^{-1} [21,22]. The spectrum corresponding to F presents the most characteristic bands present in rayon (i.e. bands A, D, I, K and L in Figure 2.b).

3.2. Thermal analysis of the reinforcing fibre

The curves in Figure 3 correspond to the decomposition of MF, F, RF and the tyre rubber (TC). The thermal decomposition of MF and RF shows three overlapping stages, while the curve corresponding to F decomposition shows two clearly differentiated steps. The curve corresponding to TC presents two main stages. The details of all of the decomposition stages are presented in Table 2. To facilitate the identification of the decomposition steps, those occurring at similar temperatures have been situated in the same row. As can be seen, TC loses 9.3 wt% of volatile matter up to 300 ℃ which is ascribed in the literature to extender oils and additives used in the preparation of the tyres [12,26]. The following steps in the thermal decomposition of TC have been assigned to the presence of natural rubber (Tmax= 378 ℃) and a blend of butadiene rubber with styrene-butadiene rubber (Tmax= 427 ℃). All the materials included in the study lose most of their volatiles in the temperature range between 300 and 500 ℃. The reinforcing fibre presents a devolatilization step at 347 ℃ which corresponds to the first step in the thermal decomposition of MF and F at temperatures of 349 and 343 ℃ respectively. The next steps in the decomposition of RF in rising order of temperature correspond to the decomposition of rubber at 382 ℃ and at 422 ℃. The latter appears also in F and in TC at 423 and 427 ℃ respectively. F shows a small

peak at 570 ℃ which could correspond to the decomposition of a high thermal stability polymer like aramid as shown by FTIR.

For the identification of MF and F the following fibres were selected: Rayon (Ra), Nylon 6 (Ny6), Nylon 6.6 (Ny6.6), polyester Dacron (Da) and aramid as indicated by the results of FTIR. The parameters derived from the decomposition test have been included in Table 3, the DTG curves have been included as Figure S1. The pure polymers present a single peak that corresponds to their complete thermal decomposition, except in the case of Ny6,6 that presents two steps. The initial and final temperatures of decomposition, $T_{i,5\%}$ and $T_{f,95\%}$ respectively, have been included in Table 3 and correspond to the temperatures at which mass losses of 5 and 95 % respectively were observed. Ra starts to decompose at a lower temperature than the other polymers 292 vs 396, 386, 382 and 524 ℃. The temperature needed to attain 95 % decomposition is also lower for Ra than for the other three polymers. The temperature of maximum volatile matter evolution of Ra is 347 ℃ (Table 3) which corresponds to the first devolatilization step of F and MF (343 and 349 ℃ respectively). Da, Ny6 and Ny6,6, present a similar temperature range of decomposition, making it more likely that interactions between them could occur. For this reason the Ny6:Da and Ny6,6:Da blends were tested. Figure 4a contains the devolatilization profile obtained for blends of Ny6 and Da in various ratios i.e. 20:80, 50:50, 70:30 and 80:20, whereas Figure 4b shows the DTG curves corresponding to the decomposition of blends of Ny6,6 and Da in various ratios i.e. 30.80, 50:50 and 70:30. The DTG curve (Figure 4a.) corresponding to the blend Ny6/Da 20:80 presents a broad band in which two maxima are visible at 397 and 426 ° C with a similar DTG value (see Table 3). Moreover the amount of volatile matter evolved up to 400 ℃, which is around 7% in the case of the single polymers, increases to nearly 22% in this blend. Therefore, the thermal decomposition of the blend occurs at a lower temperature than that of any of the pure polymers. At 450 ℃ the pure polymers have lost 60.7 and 84.5 % of their volatiles but in the case of the blends this percentage increases with the increase in Ny6 in the blends, up to 94.6% for the 50:50 blend, after which it decreases to 88.7% for the blend 80:20. At 500 ℃ the pure polymers and the blends have lost more than 90 % of

their volatile matter. Although it is evident that interaction occurs during the thermal decomposition of the blends Ny6/Da, this is not reflected in the char yield: the experimental values are similar to those calculated taking into account the blend composition and the char yield of the pure polymers. In the case of blends Ny6,6/Da (Figure 4b, Table 3) the situation is similar. The volatile matter evolved up to 400 °C increases with the amount of Da present in the blend from 30 to 70 wt% although Da evolves a lower amount of volatiles up to 400 ℃ than Ny6,6. The maximum decomposition rate for the blend Ny6,6/Da (30:70) occurs in two stages, although these take place at similar temperatures i.e. 411 and 416 ℃. Increasing the amount of Ny6,6 in the blend leads to the appearance of two decomposition steps that appear over a higher temperature range (i.e. 40 degrees in the case of the blend Ny6,6/Da 50:50 and 48 degrees in the case of the blend Ny6,6/Da 70:30). Da and Ny6,6 both present a decomposition peak at 433 ℃. In the case of blends 70:30 and 50:50, this peak disappears, while another peak appears at higher temperatures (457 and 461 ℃) indicating that some reaction occurs between the two polymers. When the percentage of Da is greater than that of Ny6,6, no reaction occurs and decomposition takes place at a lower temperature (411-416 ℃).

The interaction between the two polymers can be attributed to the fact that, during the blending of condensation polymers, chemical reactions occur that give rise to the formation of copolymers [27-31]. Compatible systems usually lead to the additivity of properties. However with incompatible polymer blends the final properties will be determined by those of the pure polymers, the geometrical arrangements of the two phases, their morphology, the extent of interpenetration and the nature of the interface [29]. Samperi [32] working with blends of Nylon-6 and Poly(ethylene terephthalate) which contain within their structure a reactive functional group, observed reactions of chemical exchange when these polymers are blended in a molten state, producing a compound with different properties. This indicates that polyester–polyamide copolymers are formed through an ester–amide interchange reaction during the melt blending of polyester and polyamide [32]. Other authors [33,34] have characterized the ester–amide interchange reaction of polyethylene

terephthalate (PET) and polyamide (PA) catalyzed by *p*-toluenesulfonic acid using DSC, 1H and 13C NMR. Yet other authors have suggested that due to the chemical structure of the PET and PA, the interaction could be a consequence of the formation of hydrogen bonding between the carbonyl group in PET and the hydrogen in the amide group in PA [35].

DSC analysis has been widely employed to characterize polymeric materials [36-41]. In order to elicit more information on the characteristics that might help to identify the various polymers that form the tyre reinforcing fibre, differential thermal analysis was performed. Figure 6 shows the variation in heat flow for the pure polymers Ny6, Ny6.6, Da and two binary blends (Ny6:Da 20:20 and Ny6,6:Da 50:50. The curves corresponding to the microfibre (MF) and the fibre (F) together with the melting temperatures have also been incorporated in the graph. Ra does not melt, it gives an endothermic peak at around 70 ℃ which corresponds to the dehydration process and another peak at a higher temperature which is related to its pyrolytic decomposition [42]. Aramid fibre was also tested but no melting was detected. The melting temperatures of Ny6, Da and Ny6,6 measured in this work were 223, 257 and 260 ℃ respectively, the associat ed enthalpies being 53.7, 43.1 and 75.2 J/g for Ny6, Da and Ny6,6. The values obtained in the present research work agree with those in the literature. Melting temperatures of 255 and 257 ℃ have been reported for Da with associated enthalpies of between 36.07 and 43.20 J/g [36-38]. Melting temperatures found in the literature for Ny6 [16, 39, 40] vary between 219 and 221 ℃. In the case of Ny6,6 the melting temperature lies between 259 and 262 ℃ [16, 40, 41].

The blend Ny6,6/Da produces a unique melting peak (Tm= 260-261 ℃) with enthalpies that increase from 29.13 to 41.83 J/g with the amount of Ny6,6 in the blend.

The blend Ny6/Da presents two endothermic peaks at almost the same temperature values as the homopolymers (see Figure 5). These results indicate that at this temperature very moderate or no reaction exchange has occurred. Similar results have been reported in the literature [32].

The DSC curve corresponding to the microfibre (MF) is similar to that of the blend Ny6/Da with two melting peaks which occur at similar temperatures. In the case of F, there is

only one melting peak at Tm= 256 ℃. Taking into consideration the results shown in Figure 2, this peak should correspond to Da. From the results derived from FTIR, thermogravimetric analysis and DSC, it can be concluded that F is composed of Da, Ra and aramid.

The results obtained from thermogravimetric analysis suggest that the microfibre includes a blend of Ny6,6 and Da. The DTG curve corresponding to the blend 70:30 has two distinct decomposition stages at 409 and 457 ℃ (Table 3) that could correspond to the last two peaks of the decomposition of the MF that occurs at around 400 and 450 ℃ (Table 3). Although some Ny6:Da blends (70:30 and 80:20) appear to present two decomposition steps at similar temperatures to MF, they are more likely to be a main decomposition stage at around 400 ℃ and a shoulder at around 450 ℃). On the other hand, the results from DSC indicate that Ny6 is the polymer that appears in the microfibre because both the Ny6:Da blend and MF present two melting peaks at the same temperatures (220 and 260 ℃). As a consequence ternary blends that included Ny6, Ny6,6 and Da were prepared. Table 4 shows the parameters derived from the thermal analysis of the blends containing Ny6,6, Ny6 and Da. The composition of the blends was adjusted to try to resemble the last two decomposition peaks of the curve corresponding to MF (Figure 4, Table 3) taking into account also the results obtained for the binary blends in Table 3. The temperature at which the decomposition of 5% of the sample ($T_{i,5\%}$) is attained is very similar for the four blends tested and very similar to that of Ny6,6 and Ny6 (i.e. 382 and 386 ℃ respectively). On the other hand, the temperature that corresponds to 95% devolatilization ($T_{i,95\%}$) is higher in the case of the blends with a higher amount of Da in their composition. The blends with the compositions Ny6,6:Ny6:Da 30:20:50 and 40:25:35 (Table 4) present two peaks which can be associated to those that appear in the decomposition of MF. The differences in the temperatures of maximum devolatilization rate (Tmax) associated to these peaks together with the relative values of the DTGmax for these peaks point to blend Ny6,6:Ny6:Da 40:25:35 as being the one which resembles last two peaks of the DTG curve of MF. The melting points of the ternary blends are very similar to those of MF (Table 4). The DTG

curves corresponding to the ternary blends have been included in the supplementary material (Figure S2).

3.3. Chromatographic analysis of the pyrolysis oils

The information derived from the study of the thermal behaviour of the selected polymers can be considered insufficient to explain the composition of the reinforcing fibre, specially to confirm the presence of Ny6 or Ny6,6 in the microfibre. Consequently the chemical composition of the volatile matter that evolves during their pyrolysis was determined by means of gas chromatography. In this way it was be possible to identify typical compounds derived from the pyrolysis of the pure polymers in the oil from the reinforcing fibre (RF). Most of the papers published deal with the oil derived from tyre crumbs [43,44] because little work has been published on the composition of the oil obtained from reinforcing fibre [9, 45]. The polymers, the microfibre and reinforcing fibre were pyrolyzed to a final temperature of 850 ℃. The oil, coke and gas yields corresponding to the pyrolysis tests carried out are shown in Table 5. Data corresponding to F have not been included considering the high contribution of rubber to its mass balance. Of the pure polymers, rayon and polyester (Da) present the highest char yield. The values obtained for RF and MF are higher due to the presence of rubber which produces a greater char yield [46]. Da produces a greater amount of gas due to the generation of CO_2 during the decomposition of the polyester [47]. The main pyrolysis product derived from the two polyamides tested is oil. The oils obtained from pyrolysis were solubilized in dichloromethane (DCM) and analysed by means of gas chromatography in order to identify the most characteristic decomposition products of the oils from the polymers present in the oil derived from the reinforcing fibre and the microfibre.

It was not our objective to make a detailed identification of the volatile compounds that are present in the oils but to identify the most characteristic decomposition products. Figure 6 shows the chromatograms corresponding to RF, MF, Da, Rayon, Ny6 and Ny6,6. The chromatograms evidence the great complexity of the oils and the difficulties involved in

identifying the compounds. The main compounds identified by means of GC-MS were included in the caption of Figure 6.

The most abundant compound in the oil derived from the reinforcing fibre was limonene ($C_{10}H_{16}$) which is a cyclic terpene that contains two units of isoprene and owes its presence in the oil to the decomposition of rubber that is present in RF. Ny6,6 decomposes to produce mainly cyclopentanone while Ny6 produces caprolactam [48]. However the thermal degradation of polyester produces CO_2 and CO, together with volatile aromatics such as toluene, biphenyl, phenanthrene and benzoic acid [50]. As in the case of cellulose, Rayon decomposes producing furan compounds such as furfural and derivatives [51].

From the total ion chromatogram (TIC) of the reinforcing fibre and the microfibre selected ions, characteristic of the decomposition of the pure polymers, were extracted (Figure S3). Cyclopentanone (m/z=84) and caprolactam (m/z=113) obtained from the polyamides; furfural (m/z=96) and methylfurfural (m/z=110) derived from the decomposition of rayon; and benzoic acid (m/z=122) and biphenyl (m/z=154) characteristic of the decomposition of Da. The presence of these products confirms that Ny6,6, Ny6, Da, and Ra are present in the composition of the MF.

4. Conclusions

Waste reinforcing fibre is composed of two cords of different composition (F and MF) taking into account their different mechanical behaviour in the process of size reduction of scrap tyres. FTIR was useful to reveal the polymers that were present in the waste reinforcing fibre. Thermal analysis showed that the microfibre (MF) was composed mainly of Ra, Da, Ny6,6 and Ny6. DSC revealed the presence of two melting peaks corresponding to the blend of Da, Ny6,6 and Ny6. Ra did not show any melting peak when DSC was used. From the FTIR results and thermal analysis it was concluded that F, included aramid, Da and Ra. Pyrolysis of the waste reinforcing fibre was carried out and the oil obtained analysed and compared to that derived from the pure polymers in order to confirm the presence of Ny6 and Ny6,6 in the microfibre. It was found that the main decomposition compounds from the pure polymers were present in the pyrolysis oil of the reinforcing fibre. The results indicate that

Ny6,6 and Ny6 are both present in the microfibre. It can be concluded that the reinforcing fibre is composed of Ny6,6, Ny6, Da and Ra (MF) and Ra, Da and aramid (F). The procedure here explained to identify polymers in a blend, can be useful to identify the components of other blends.

Ackowledgements

The research leading to these results has received funding from the Spanish MICINN project reference CTM2009-10227. BA. thanks the Government of the Principado de Asturias for the award of a predoctoral grant with funds from PCTI-Asturias.

References

[1] V. Sahajwalla, M. Zaharia, M. Rahman, R. Khanna, N. Saha-Chaudhury, P. O'Kane, J. Dicker, C. Skidmore, D. Knights, Recycling rubber tyres and waste plastics in EAF steelmaking, Steel research International 82 (2011) 566-572.

[2] G. Ramos, F.J. Alguacil, F.A. López, The reclycing of end-of-life tyres. Technological review, Revista de metalurgia 47 (2011) 273-284.

[3] W.S. Anthony, Separation of Crumb and Fiber in Tire Recycling Operations, ASAE Annual International Meeting 2005; Paper Number: 056139.

[4] T. Amari, N.J. Themelis, I.K. Wernick, Resource recovery from used rubber tires, Resources Policy 25 (1999) 179-188.

[5] M. Kyari, A. Cunliffe, P.T. Williams, Characterization of oils, gases and char in relation to the pyrolysis of different brands of scrap automotive tires, Energy Fuels 19 (2005) 1165-1173.

[6] R. Murillo, E. Aylón, M.V. Navarro, M.S. Callén, A. Aranda, A.M. Mastral, The application of thermal processes to valorise waste tyre, Fuel Process Technol 87 (2006) 143-147.

[7] G. San Miguel, G.D. Fowler, Ch.J. Sollars, A study of the characteristics of activated carbons produced by steam and carbon dioxide activation of waste tyre rubber, Carbon 41 (2003) 1009-1016.

[8] C. Díez, O. Martínez, L.F. Calvo, J Cara, A. Morán, Pyrolysis of tyres, Influence of the final temperature of the process on emissions and the calorific value of the products recovered, Waste Manage 24(2004) 463-469.

[9] A.M. Fernández, C. Barriocanal, R. Alvarez, Pyrolysis of a waste from the grinding of scrap tyres, J Hazard Mater 203-204 (2012) 236– 243.

[10] I. De Marco, M.F. Laresgoiti, M.A. Cabrero, A. Torres, M.J. Chomón, B. Caballero, Pyrolysis of scrap tyres, Fuel Process Technol. 72 (2001) 9-22.

[11] C. Roy, A. Chaala, H. Darmstadt, Vacuum pyrolysis of used tyres end-uses for oil and carbon black products, J Anal Appl Pyrolysis 51 (1999) 201-221.

[12] S. Seidelt, M. Müller-Hagedorn, H. Bockhorn H, Description of tire pyrolysis by thermal degradation behaviour of main components, J Anal Appl Pyrolysis 75 (2006) 11-18.

[13] P.T. Williams, S. Besler, Pyrolysis-thermogravimetric analysis of tyres and tyre components, Fuel Process Technol 74 (1995) 1277-1283.

[14] J. Yang, S. Kaliaguine, C. Roy, Improved quantitative determination of elastomers in tire rubber by kinetic simulation of DTG curves, Rubber Chem. and Technol. 66 (1993) 213-229.

[15] A.K. Naskar, A.K. Mukherjee, R. Mukhopadhyay, Studies on tyre cords: degradation of polyester due to fatigue, Polym Degrad. Stab. 83 (2004) 173-180.

[16] F. Parres, J.E. Crespo-Amorós, A. Nadal-Gisbert, Mechanical properties analysis of plaster reinforced with fiber and microfiber obtained from shredded tires, Constr Build Mater 23 (2009) 3182-3188.

[17] F. Parres, J.E. Crespo-Amorós, A. Nadal-Gisbert, Characterization of fibers obtained from shredded tires, J Appl Polym Sci 113 (2009) 2136-2142.

[18] A. Bartl, A. Hackl, B. Mihalyi, M. Wistuba, I. Marini, Recycling of fibre materials, Trans IChemE, Part B, Process Saf Environ Prot 83 (2005) 351–358.

[19] B. Smith, editor. Infrared Spectral Interpretation: a systematic approach. Boca Raton: CRC Press, 1998.

[20] F. Carrillo, X. Coloma, J.J. Suñol, J. Saurina, Structural FTIR analysis and thermal characterisation of lyocell and viscose-type fibres, Eur Polym J 40 (2004) 2229–2234.

[21] S.Y. Oh, D. Yoo, Y. Shinb, G. Seo, FTIR analysis of cellulose treated with sodium hydroxide and carbon dioxide, Carbohydr Res 340 (2005) 417–428.

[22] L.M. Proniewicz, C. Paluszkiewicz, A. Wesełucha-Birczyńska, H. Majcherczyk, A. Barański, A. Konieczna, FT-IR and FT-Raman study of hydrothermally degradated cellulose, J Mol Structure 596 (2001) 163-169.

[23] R.J. Morgan, N.L. Butler, Hydrolytic degradation mechanism of Kevlar 49 fibers when dissolved in sulfuric acid, Polym Bull 27 (1992) 689-696.

[24] E.Y. Kim, S.K. An, H.D. Kim, Graft Copolymerization of e-Caprolactam onto Kevlar-49 Fiber Surface and Properties of Grafted Kevlar Fiber Reinforced Composite, J Appl Polym Sci 65 (1997) 99–107.

[25] R. Ou, H. Zhao S. Sui, Y. Song, Q. Wang, Reinforcing effects of Kevlar fiber on the mechanical properties of wood-flour/high-density-polyethylene composites. Composites: Part A 41 (2010) 1272–1278.

[26] M.B. Larsen, L. Schultz, P. Glarborg, L. Skaarup-Jensen, K. Dam-Johansen,F. Frandsen, U. Henriksen, Devolatilization characteristics of large particles of tyre rubber under combustion conditions, Fuel 85 (2006) 1335–1345.

[27] K. Ch. Chiou, F. Ch. Chang, Reactive compatibilization of polyamide-6 (PA 6)/Polybutylene terephthalate (PBT) blends by a multifunctional epoxy resin, J Polym Sci: Part B: Polym Phsys 38 (2000) 23-33.

[28] B. Yilmaz, Investigation of Twisted Monofilament Cord Properties Made of Nylon 6.6 and Polyester, Fiber Polym 12 (2011) 1091-1098.

[29] L.A. Utracki, A.M. Catani, G.L. Bata, M.R. Kamal, V. Tan, Melt rheology of blends of semicrystalline polymers. I. Degradation and viscosity of Poly(ethylene terephthalate)-Polyamide-66 mixtures, J Appl Polym Sci 27 (1982) 1913-1931.

[30] M. Shen, H. Kawai, Properties and structure of polymeric alloys, AIChE J 24 (1978) 1-20.

[31] S. Fakirov, M. Evstatiev, M. Schultz, Microfibrillar reinforced composite from drawn poly(ethylene terephthalate)/nylon-6 blend, Polymer 34 (1993) 4669-4679.

[32] F. Samperi, C. Puglisi C, R. Alicata, G. Montando, Essential role of chain ends in the Nylon-6/Poy(ethylene terephthalate) exchange, J Polym Sci: Part A: Polym Chem 41 (2003) 2778-2793.

[33] L.Z. Pillon, L.A. Utracki, Compatibilization of polyester/polyamide blends via catalytic ester-amide interchange reaction, Polym Eng Sci 24 (1984) 1300-1305.

[34] L.Z. Pillon, J. Lara, D. W. Pillon, On the crystallinity and some structure/property relationships of poly(ethylene terephthalate)-poly(amide-6,6) blends, Polym Eng Sci 27 (1987) 984-989.

[35] L.Z. Pillon, L.A. Utracki, Spectroscopic study of Poly(ethylene Terephthalate)/Poly(amide-6.6) blends, Polym Eng Sci 27 (1987) 562-567.

[36] Y. Wang, J. Gao , Y. Ma, U.S. Agarwal, Study on mechanical properties, thermal stability and crystallization behaviour of PET/MMT nanocomposites, Composites: Part B 37 (2006) 399-407.

[37] M. Jayakannan, S. Ramakrishnan, Synthesis and thermal analysis of branched and “kinked” poly(ethylene terephthalate), J Polym Sci: Part A: Polym Chem 36 (1998) 309-317.

[38] R. Séguéla, Temperature dependence of the melting enthalpy of poly(ethylene terephthalate) and poly(aryl-ether-ether-ketone), Polymer 34 (1993) 1761-1764.

[39] J.W. Cho, D.R. Paul, Nylon 6 nanocomposites by melt compounding, Polymer 42 (2001) 1083-1094.

[40] P.R. Hornsby, J. Wang, R. Rothon, G. Jackson, G. Wilkinson, K. Cossick, Thermal decomposition behaviour of polyamide fire-retardant compositions containing magnesium hydroxide filler, Polym Degrad Stab 51 (1996) 235-249.

[41] W. Qiu, A. Habenschuss, B. Wunderlich, The phase structures of nylon 6.6 as studied by temperature-modulated calorimetry and their link to X-ray structure and molecular motion, Polymer 48 (2007) 1641-1650.

[42] A.C. Pastor, F. Rodríguez-Reinoso, H. Marsh H, M.A. Martínez, Preparation of activated carbon cloths from viscous rayon. Part I. Carbonization procedures, Carbon 37 (1999) 1275–1283.

[43] M. R. Islam, M.S.H.K. Tushar, H. Haniu. Production of liquid fuels and chemicals from pyrolysisof Bangladeshi bicycle/rickshaw tire wastes. J. Anal. Appl. Pyrolysis 82 (2008) 96–109.

[44] M.F. Laresgoiti, B.M. Caballero, I. de Marco, A. Torres, M.A. Cabrero, M.J. Chomón. Characterization of the liquid products obtained in tyre pyrolysis. J. Anal. Appl. Pyrolysis 71 (2004) 917–934.

[45] B. Acevedo, C. Barriocanal. Fuel-oils from co-pyrolysis of scrap tyres with coal and a bituminous waste. Influence of oven configuration. Fuel 125 (2014) 155-163.

[46] B. Acevedo, C. Barriocanal, R. Alvarez, Pyrolysis of blends of coal and tyre wastes in a fixed bed reactor and a rotary oven, Fuel 113 (2013) 817-825.

[47] T Yoshioka, G. Grauseb, C. Egerb, W. Kaminsky, A. Okuwaki, Pyrolysis of poly(ethylene terephthalate) in a fluidised bed plant. Polymer Degradation and Stability 86 (2004) 499-504.

[48] M. Herrera, G. Matuschek, A. Kettrup, Main products and kinetics of the thermal degradation of polyamides,Chemosphere 42 (2001) 601-607.

[49] A. Ballistreri, D. Garozzo, M. Giuffrida, G. Impallomeni, G. Montaudo, Primarry thermal docomposition processes in aliphatic polyamides, Polymer Degradation adn Stability 23 (1988) 25-41.

[50] Samperi, C. Puglisi, R. Alicata, G. Montaudo, Thermal degradation of poly(ethylene terephthalate) at the processing temperature, Polymer Degradation and Stability 83 (2004) 3–10

[51] Q. Lu, X. Yanga, Ch. Donga, Z. Zhanga, X. Zhanga, X. Zhub. Influence of pyrolysis temperature and time on the cellulose fast pyrolysis products: Analytical Py-GC/MS study. J. Anal. Appl Pyrol. 92 (2011) 430–438.

Table 1. Main characteristics of the raw materials.

	TC	F	MF	RF[d]
VM[a] (wt.% db[b])	65.5	66.5 [e]	80.4 [e]	72.9
Ash(wt.% db)	7.5	6.0[f]	3.0 [f]	4.6
C (wt.% db)	78.5	77.6	57.2	68.2
H (wt.% db)	7.0	7.0	6.3	6.7
N (wt.% db)	1.3	0.4	2.0	1.1
S (wt.% db)	2.13	1.48	0.51	1.03
O (wt.% db)	3.9	7.8	31.2	18.6
C/H[c]	0.93	0.92	0.76	0.85

a: volatile matter (ISO562), b: dry basis, c: atomic ratio, d: calculated from the data of F and MF considering 54 wt% of F and 46 wt% of MF, e: from thermogravimetric analysis.

Table 2. Parameters derived from the thermogravimetric analysis of F, MF, RF and TC.

	F	MF	RF	TC
MV300[a]	8.1	3.4	8.3	9.3
MV400[a]	62.5	50.7	59.8	52.3
MV500[a]	94.3	97.4	95.5	94.9
T1 max[c] (ºC)	343	349	347	--
DTGmax1[b] (%/min)	9.00	4.20	4.33	--
T2 max[c] (ºC)	--	396	382	378
DTGmax2[b] (%/min)	--	8.93	5.43	4.95
T3 max[c] (ºC)	423	444	422	427
DTGmax3[b] (%/min)	7.42	5.90	4.33	4.45
T4 max[c] (ºC)	570	--	--	--
DTGmax4[b] (%/min)	0.23	--	--	--
CY[d](%)	12.8	11.5	27.7	34.3

[a]VMT: volatile matter evolved up to a specific temperature (T) and normalized to 100 %.
[b] DTGmax: Rate of maximum volatile matter evolution.
[c] Tmax: Temperature of maximum volatile matter evolution.
[d] CY: Char yield at 950 ℃.

Table 3. Parameters derived from the thermal decomposition of the polymers and different blends of the polymers selected as components of the microfibre and fibre.

	Rayon	Da	Ny6	Ny6,6	Aramid	Ny6:Da 20:80	Ny6:Da 50:50	Ny6:Da 70:30	Ny6:Da 80:20	Ny6,6:Da 70:30	Ny6,6:Da 50:50	Ny6,6:Da 30:70
$T_{i,\ 5\%}$ (℃)	292	396	386	382	524	385	383	377	384	394	392	3 90
$T_{f,\ 95\%}$ (℃)	443	495	471	463	709	467	454	459	462	474	474	4 76
MV300[a]	6.84	0	0	0	1.4	0	0	0	0	0	0	0
MV400[a]	93.4	6.6	8.2	17.7	2.5	21.4	32.4	39.1	21.7	8.6	11.9	15.3
MV450	95.2	84.5	60.7	85.9		90.2	94.6	92.8	88.7	70.7	77.8	89.4
MV500[a]	96.6	95.2	99.7	99.3	3.0	96.8	97.4	98.6	99.2	98.9	98.4	96.9
T1 max[c] (ºC)	347	433	453	418	--	397	401	402	407	409	421	411
DTGmax1[b] (%/min)	24.44	19.36	19.93	16.55	--	12.40	27.09	30.18	25.65	17.07	16.15	22.50
T2 max[c] (ºC)	--	--	--	433	--	426	409	452	448	457	461	416
DTGmax2[b] (%/min)	--	--	--	15.68	--	13.91	23.94	2.43	5.50	11.47	7.13	21.80
T3 max[c] (ºC)	--	--	--	--	581	--	--	--	--		--	--
DTGmax3[b] (%/min)	--	--	--	--	21.43	--	--	--	--		--	--
CY[d](%)	7.7	17.8	1.7	3.1	35.8	14.7	10.5	5.6	4.3	5.9	9.7	11.6

[a]VMT: volatile matter evolved up to a specific temperature (T) and normalized to 100 %.
[b] DTGmax: Rate of maximum volatile matter evolution.
[c] Tmax: Temperature of maximum volatile matter evolution.
[d] CY: Char yield at 950 ℃

Table 4. Parameters derived from the thermal analysis of ternary blends.

	Ny6,6:Ny6:Da 50:20:30	Ny6,6:Ny6:Da 20:50:30	Ny6,6:Ny6:Da 30:20:50	Ny6,6:Ny6:Da 40:25:35
$T_{i,\ 5\%}$ (℃)	386	385	383	386
$T_{f,\ 95\%}$ (℃)	473	467	481	471
MV300[a]	0.71	0.52	0.63	0.92
MV400[a]	15.4	21.5	21.6	18.2
MV450	72.9	84.3	86.0	77.5
MV500[a]	98.7	98.7	96.0	98.1
T1 max[c] (ºC)	403	404	413	405
DTGmax1[b] (%/min)	17.55	23.37	21.75	20.46
T2 max[c] (ºC)	408	409	--	--
DTGmax2[b] (%/min)	16.88	22.79	--	--
T3 max[c] (ºC)	455	452	453	456
DTGmax3[b] (%/min)	10.25	6.83	3.80	8.69
CY[d](%)	5.2	4.3	10.2	5.8
Tm1[e] (℃)	222	224	218	217
ΔHm1 (J/g)	10.84	28.58	12.59	16.12
Tm2[e] (℃)	260	260	257	257
ΔHm2 (J/g)	32.69	14.48	35.18	36.05

[a]VMT: volatile matter evolved up to a specific temperature (T) and normalized to 100 %.
[b] DTGmax: Rate of maximum volatile matter evolution.
[c] Tmax: Temperature of maximum volatile matter evolution.
[d] CY: Char yield at 950 ℃.
[e]Tm: melting temperature.
[f] ΔHm: Enthalpy of melting.

Table 5. Pyrolysis yield of the polymers, reinforcing fibre and microfibre.

	Rayon	Da	Ny 6	Ny 6,6	RF	MF
Char	18	22	7	13	30	30
Tar	64	44	89	73	56	49
Gas	18	34	4	14	14	21

Figure 1. Photograph of the fibre (F) a) and microfibre (MF) b) that constitute the reinforcing fibre (RF) obtained in the process of size reduction of tyres.

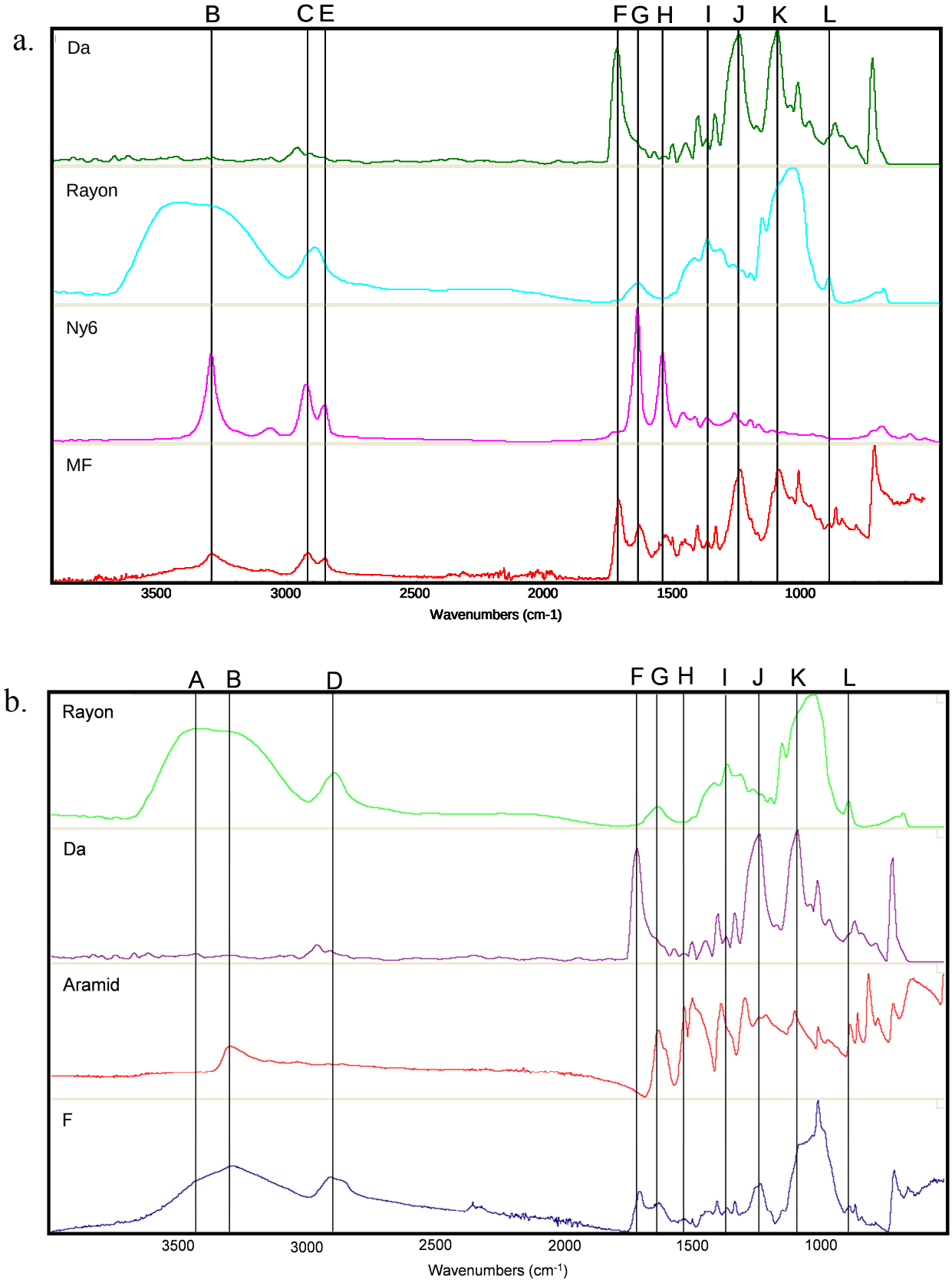

Figure 2. FTIR-ATR spectra corresponding to the pure polymers, a) MF and b) F.

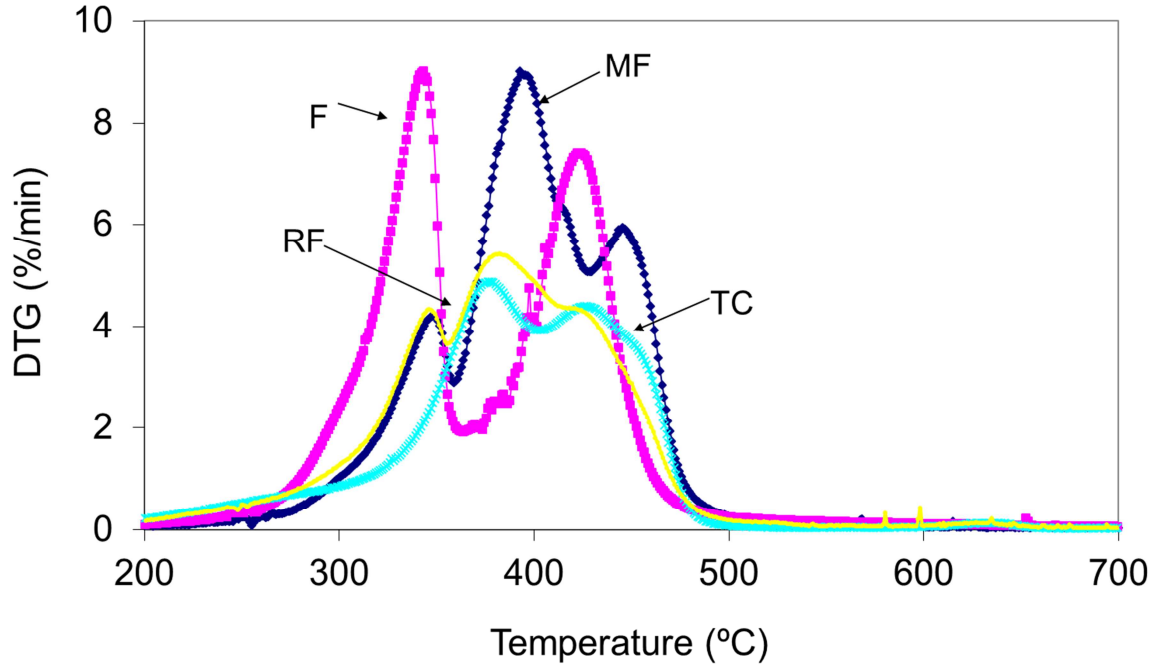

Figure 3. Derivative of the mass loss curve corresponding to the microfibre (MF), the fibre (F), the reinforcing fibre (RF) and the rubber (TC).

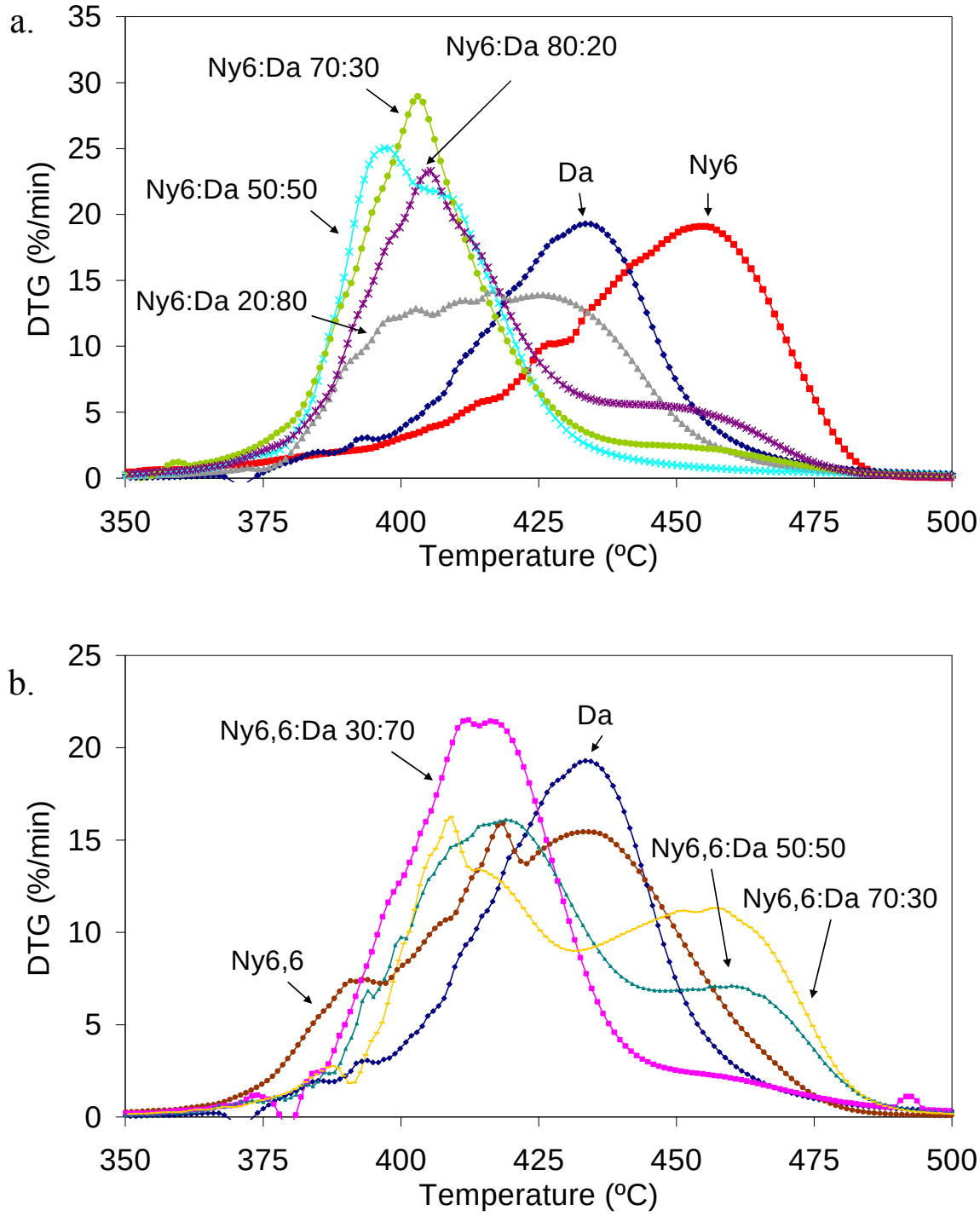

Figure 4. DTG curves of blends of (a) Da and Ny6 and (b) Da and Ny6,6.

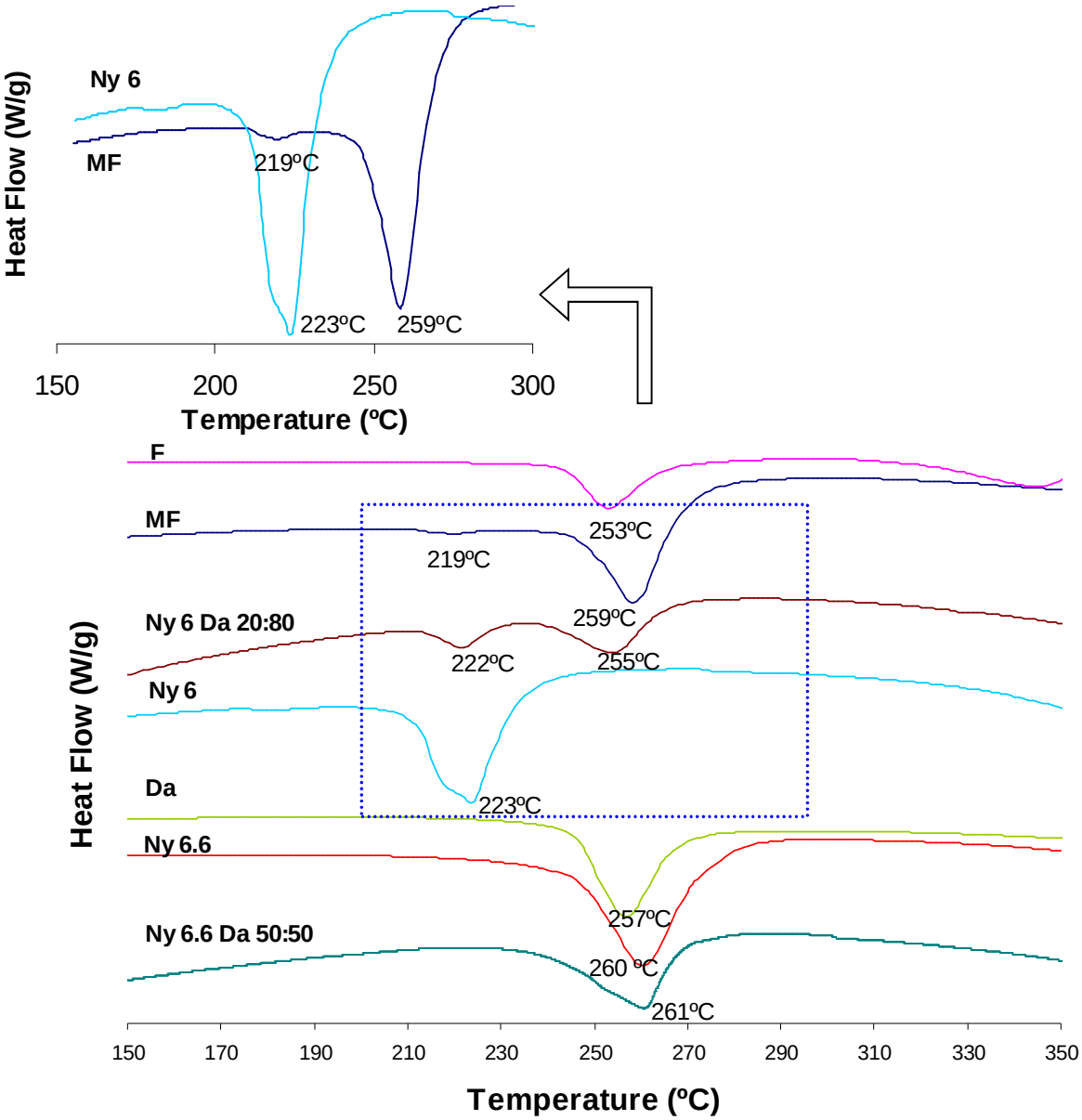

Figura 5. DSC curves corresponding to MF, F, Da, Ny6 and their blends.

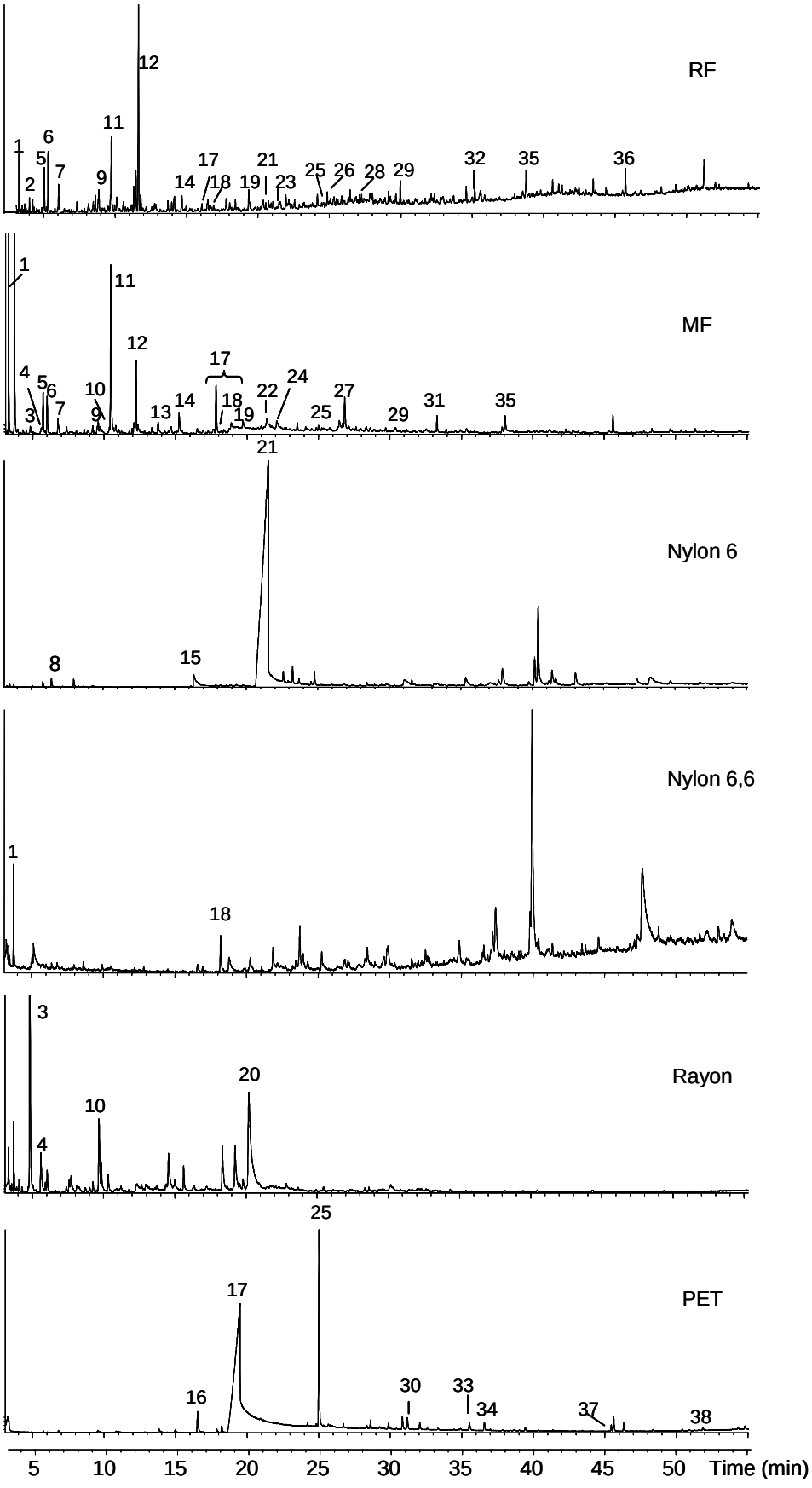
RF
MF
Nylon 6
Nylon 6,6
Rayon
PET
Time (min)

Figure 6. TIC chromatograms of RF, MF and pure polymers. 1: cyclopentanone; 2: dimethylcyclohexene; 3: furfural; 4: furanmethanol; 5: ethylbenzene; 6: xylene; 7: styrene; 8: hexanitrile; 9: ethylmethylbenzene; 10: methylfurfural; 11: benzonitrile; 12: limonene; 13: acetophenone; 14: methylbenzonitrile; 15: aminohexanitrile; 16: benzoyl isothiocyanate; 17: benzoic acid and derivatives; 18: naphthalene; 19: benzothiazole; 20: hydroxymethyl furancarboxaldehyde; 21: caprolactam; 22: benzenedicarbonitrile; 23: methylnaphthalene; 24: ethylmethylbenzoate; 25: biphenyl; 26: dimethylnaphthalene; 27: ethyl cyanobenzoate; 28: dimethylquinoline; 29: trimethylnaphthalene; 30: fluorene; 31: benzenedicarboxylic acid, diethyl ester; 32: heptadecane; 33: fluorenone; 34: phenanthrene; 35: N-hexylbenzamide; 36: heptadecanonitrile; 37: terphenyl; 38: triphenylene.

IDENTIFICATION OF POLYMERS IN WASTE TYRE REINFORCING FIBRE BY THERMAL ANALYSIS AND PYROLYSIS

B.Acevedo, A.M. Fernández, C. Barriocanal*
Instituto Nacional del Carbón, INCAR-CSIC, Apartado 73, 33080 Oviedo. Spain
*Corresponding author. Tel: +34 985 11 90 90; Fax:+34 985 29 76 62; e.mail address: carmenbr@incar.csic.es

3. Results and discussion

Table S1. Elemental analysis of F and MF free of rubber.

	F	MF
C (wt.% db)	57.7	47.8
H (wt.% db)	5.3	6.6
N (wt.% db)	0.7	2.5
O (wt.% db)	38.2	37.5
C/H[a]	0.9	0.6

a: atomic ratio

Table S2. Assignement of IR bands.

Band position (cm^{-1})	Assignment of spectral bands	Assignment in Figures 7, 8 and 9
3500-3200	v O-H	A
3301	v N-H	B
2922	v_{as} $–CH_2-$	C
2990-2795	v aliphatic C-H	D
2855	v_s $–CH_2-$	E
1720	v –C=O	F
1640	Conjugated –C=O	G
1544	σ N-H	H
1375	σ O-H	I
1245	v C-C-O	J
1100	v C-C-O	K
895	ρ CH_2	L

v – stretching vibration, σ – bending vibration, ρ – rocking vibration, s – symmetrical, as- asymmetrical,

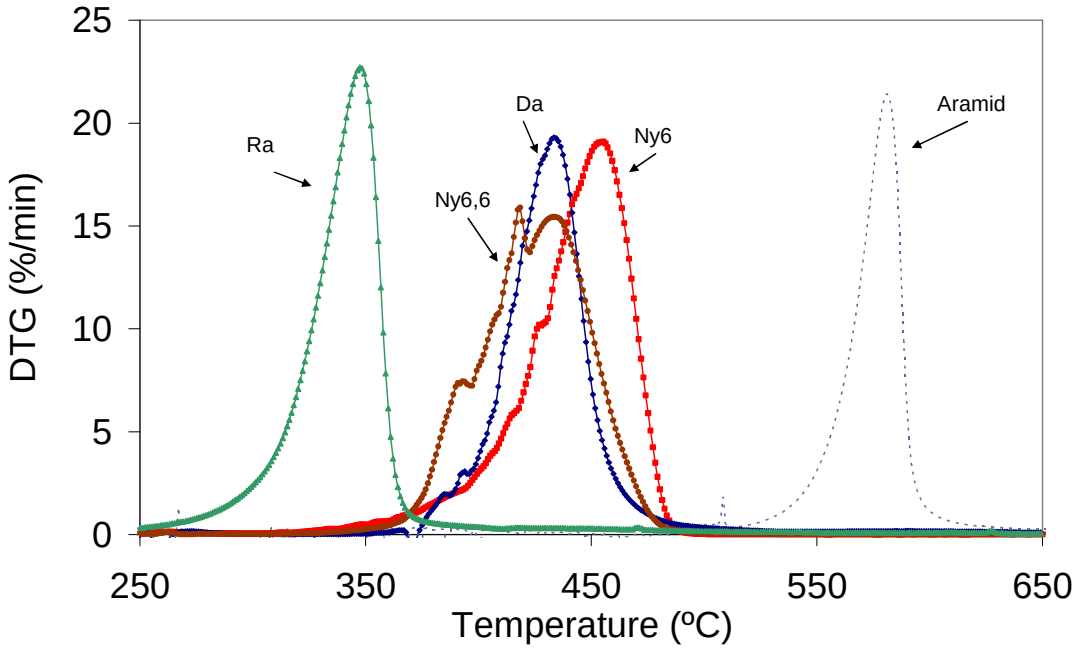

Figure S1. DTG curve corresponding to the pure polymers.

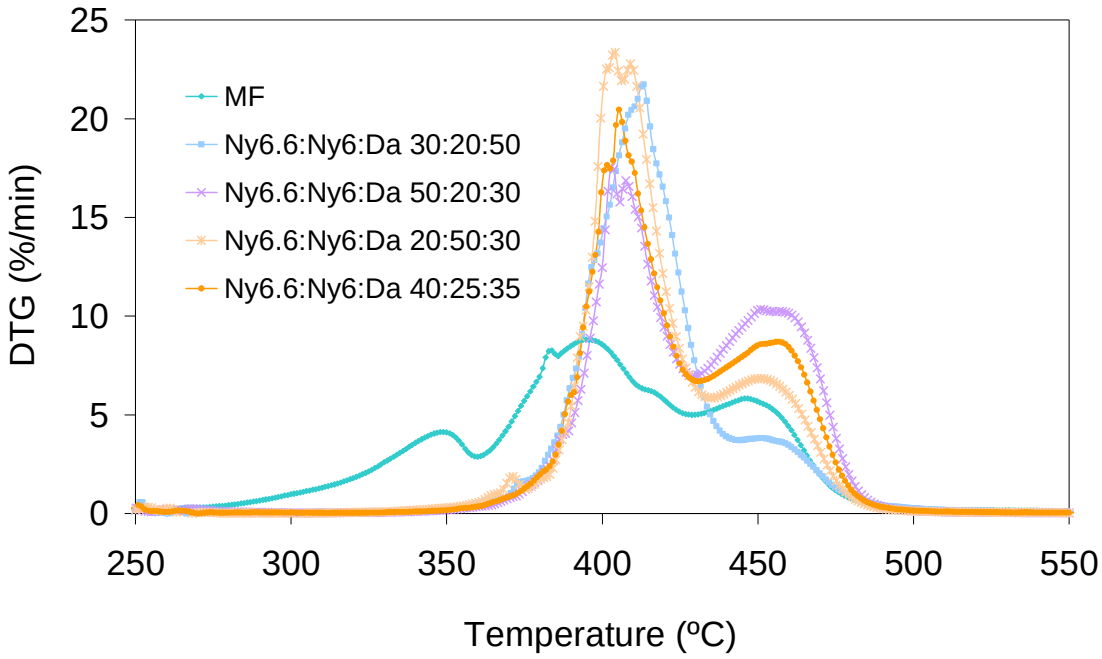

Figure S2. DTG curves corresponding to the ternary blends.

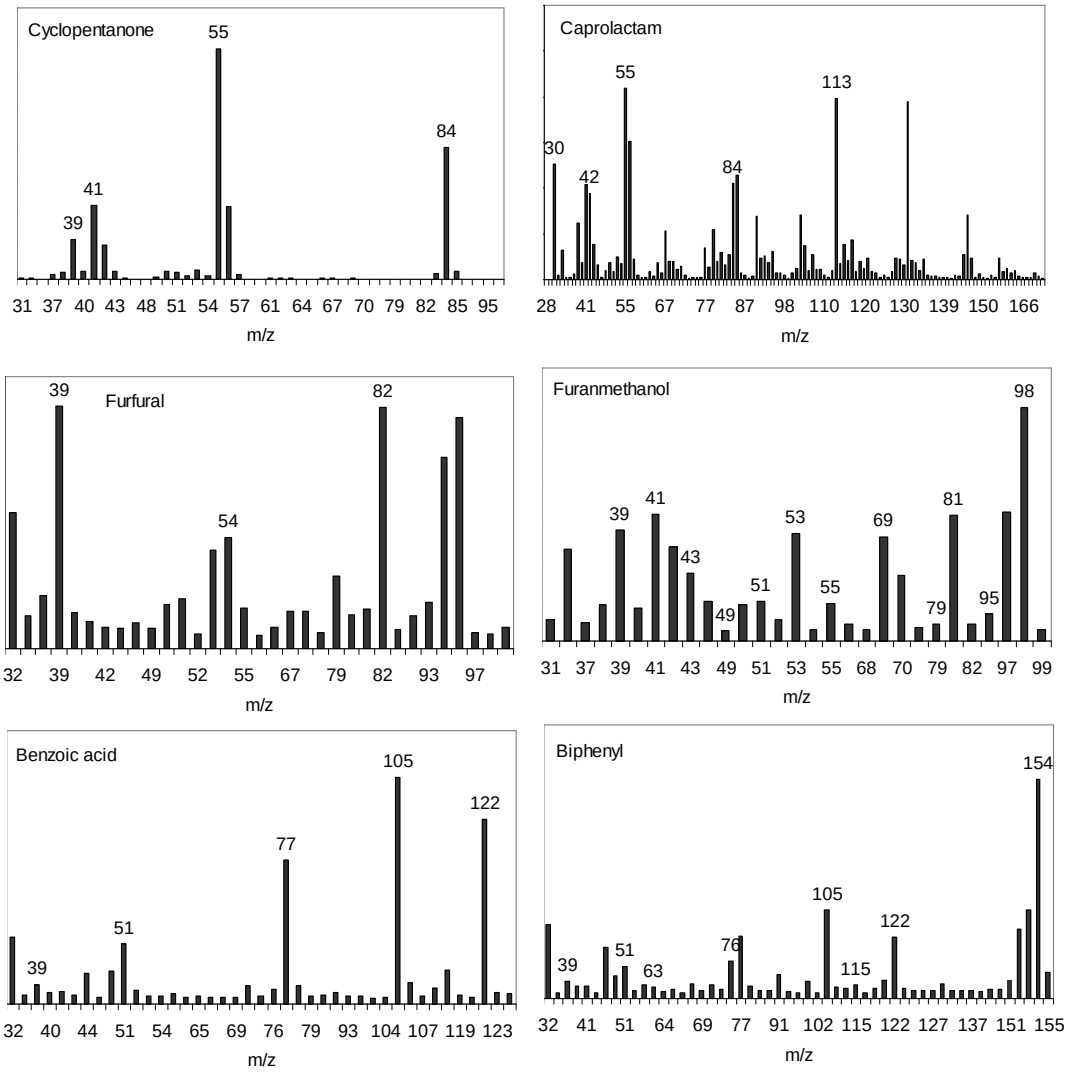

Figure S3 . Ions extracted from the TIC chromatogram of RF and MF.

Taking into consideration all the results presented here, an attempt was made to resemble the DTG profile of MF and F. In the case of the MF the DTG curve corresponding to the ternary blend 40:25:35 (Ny6,6:Ny6:Da) appeared to fit the last two peaks of the devolatilization profile of MF. The first peak in the DTG profile of MF should correspond to Ra. Then, considering the DTGmax values of the ternary blend and that of Ra (Tables 3 and 4) a mixture 80:20 was tested, the DTG profile of this mixture compared with that of F is shown in Figure S4. In the case of F, the char yield of pure polymers together with the DTGmax of the decomposition stages were considered to find that F can be composed of a 1:1 blend of Ra and Da with a small contribution of aramid (1%) (see Figure S4).

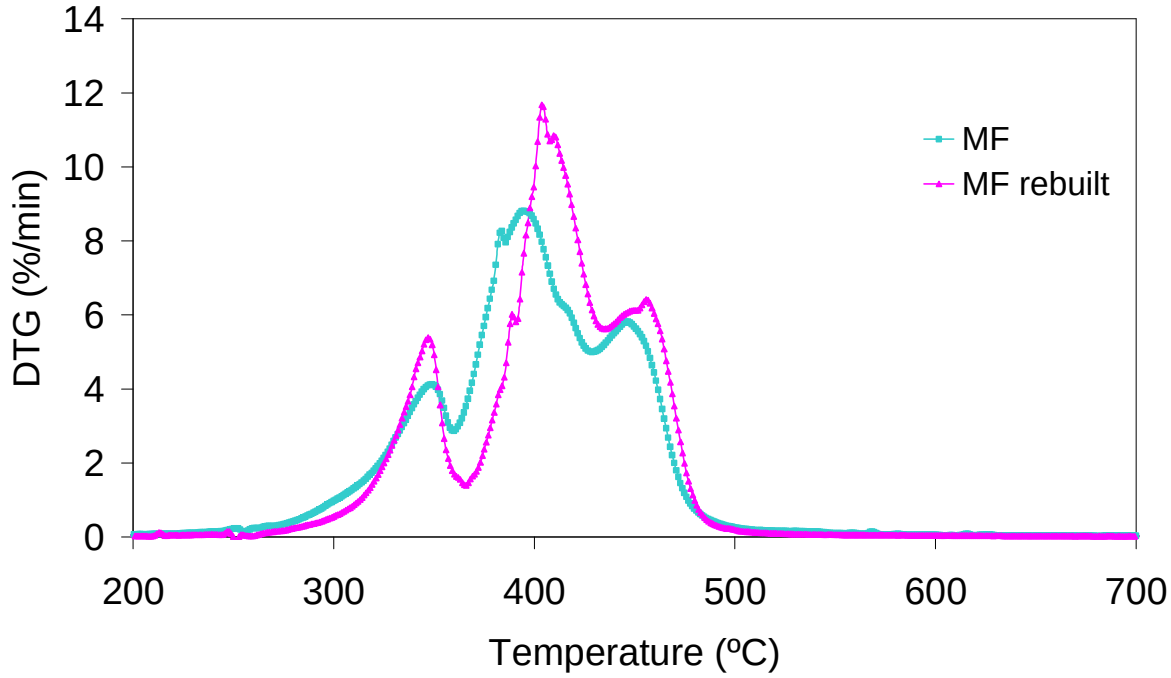

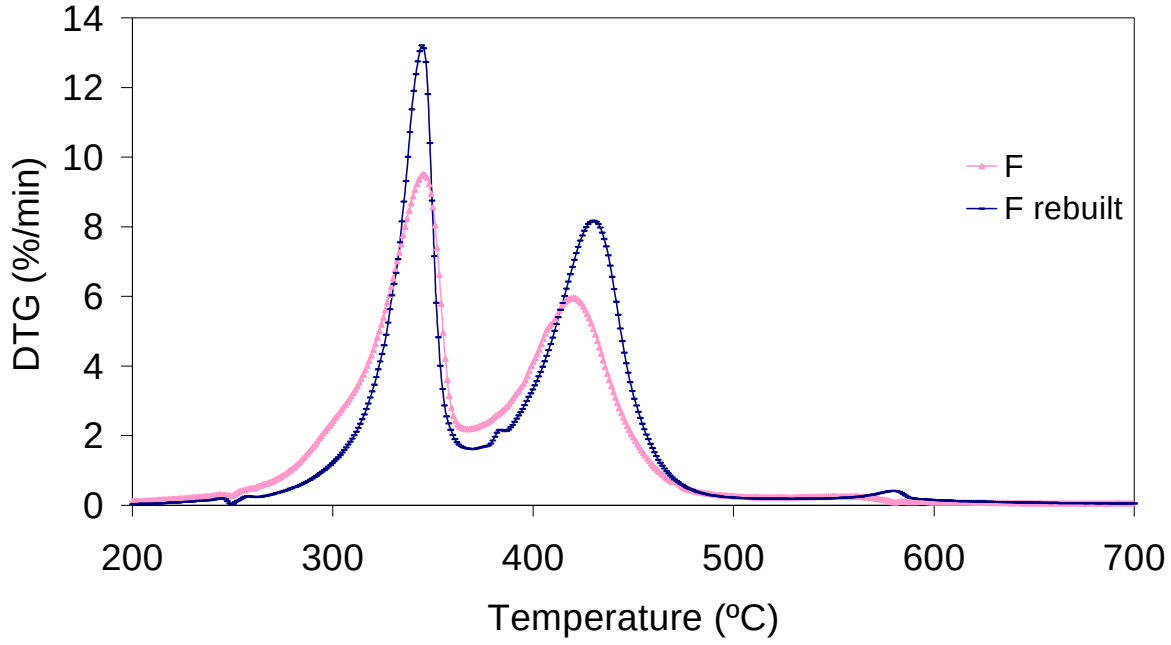

Figure S4 Comparison between the DTG curves corresponding to MF and F prepared with blends of pure polymers and those obtained from the decomposition of MF and F separated from RF.